



Structural connectivity from DTI to predict mild cognitive impairment in de novo Parkinson's disease

Xiaofei Huang^{a,1}, Qing He^{a,1}, Xiuhang Ruan^a, Yuting Li^{a,b}, Zhanyu Kuang^a, Mengfan Wang^a, Riyu Guo^a, Shuwen Bu^a, Zhaoxiu Wang^a, Shaode Yu^{c,*}, Amei Chen^{a,*}, Xinhua Wei^{a,*}

^a Department of Radiology, the Second Affiliated Hospital, School of Medicine, South China University of Technology, Guangdong, China

^b Affiliated Dongguan Hospital, Southern Medical University (Dongguan People's Hospital), Guangdong, China

^c School of Information and Communication Engineering, Communication University of China, Beijing, China

ARTICLE INFO

Keywords:

Parkinson's disease
Mild cognitive impairment
Structural connectivity
Diffusion tensor imaging
Machine learning

ABSTRACT

Background: Early detection of Parkinson's disease (PD) patients at high risk for mild cognitive impairment (MCI) can help with timely intervention. White matter structural connectivity is considered an early and sensitive indicator of neurodegenerative disease.

Objectives: To investigate whether baseline white matter structural connectivity features from diffusion tensor imaging (DTI) of de novo PD patients can help predict PD-MCI conversion at an individual level using machine learning methods.

Methods: We included 90 de novo PD patients who underwent DTI and 3D T1-weighted imaging. Elastic net-based feature consensus ranking (ENFCR) was used with 1000 random training sets to select clinical and structural connectivity features. Linear discrimination analysis (LDA), support vector machine (SVM), K-nearest neighbor (KNN) and naïve Bayes (NB) classifiers were trained based on features selected more than 500 times. The area under the ROC curve (AUC), accuracy (ACC), sensitivity (SEN) and specificity (SPE) were used to evaluate model performance.

Results: A total of 57 PD patients were classified as PD-MCI nonconverters, and 33 PD patients were classified as PD-MCI converters. The models trained with clinical data showed moderate performance (AUC range: 0.62–0.68; ACC range: 0.63–0.77; SEN range: 0.45–0.66; SPE range: 0.64–0.84). Models trained with structural connectivity (AUC range, 0.81–0.84; ACC range, 0.75–0.86; SEN range, 0.77–0.91; SPE range, 0.71–0.88) performed similar to models that were trained with both clinical and structural connectivity data (AUC range, 0.81–0.85; ACC range, 0.74–0.85; SEN range, 0.79–0.91; SPE range, 0.70–0.89).

Conclusions: Baseline white matter structural connectivity from DTI is helpful in predicting future MCI conversion in de novo PD patients.

1. Introduction

Cognitive impairment is one of the most common and important nonmotor symptoms of Parkinson's disease (PD) (Aarsland et al., 2017; Weintraub and Burn, 2011). Mild cognitive impairment (MCI) is thought to be a transition stage between normal cognition and dementia (Caviness et al., 2007). PD-MCI is a reported risk indicator for PD dementia (PDD), which occurs in nearly 80 % of de novo PD patients within 20 years and severely affects the quality of life of patients (Hely et al., 2008; Pigott et al., 2015). Therefore, it is important to identify patients with a

high risk of developing PD-MCI in the early stage of PD and elucidate its pathophysiology to enable timely intervention and delay cognitive decline.

Although some clinical and imaging biomarkers for PD-MCI have been reported, the search for more reliable biomarkers is still ongoing (Delgado-Alvarado et al., 2016). Compared to other biomarkers, neuroimaging biomarkers are more objective indicators that can provide a comprehensive view of changes in the structure and function of the brain and reveal some of the underlying pathophysiology mechanisms. Most previous studies have used neuroimaging indicators that reflect

* Corresponding authors.

E-mail addresses: yushaodemia@163.com (S. Yu), eychenamei@scut.edu.cn (A. Chen), eyxinhuawei@scut.edu.cn (X. Wei).

¹ Xiaofei Huang, Qing He contributed equally to this article and should be considered co-first authors.

baseline brain gray matter changes, including temporal, parietal, occipital and hippocampal volumes, to predict PD-MCI, while fewer studies have used white matter indicators (Caspell-Garcia et al., 2017; Filippi et al., 2020; Foo et al., 2017; Zhou et al., 2020).

Notably, several studies have reported that axonal degeneration occurs prior to cell death in patients with PD (Burke and O'Malley, 2013; Kurowska et al., 2016). Furthermore, some studies have shown that the integrity of the white matter (WM) is impaired prior to the thinning of the cortex, as evidenced by magnetic resonance imaging (MRI) results (Park et al., 2022; Rektor et al., 2018). Structural connectivity between brain regions from diffusion tensor imaging (DTI) is an important indicator of WM integrity and is thought to be associated with neuroinflammation, α -syn propagation and neuronal loss (Yau et al., 2018; Yu et al., 2020a). According to a recent review, structural connectivity is crucial for preserving the integrity and function of remote brain regions (Thiebaut de Schotten and Forkel, 2022). Some studies have used structural connectivity to build cognitive-related diagnostic and predictive models, achieving good performance (Huang et al., 2021; Lin et al., 2021; Yu et al., 2020a). However, no previous studies have used baseline structural connectivity to predict PD-MCI in newly diagnosed PD patients.

In contrast to conventional statistical methods, machine learning-based approaches can handle highly dimensional and complicated data and be used to develop diagnostic and predictive models for diseases at the individual level (Mei et al., 2021; Yu et al., 2020a). The aim of this study was to develop a machine learning model to predict the conversion risk of PD-MCI among de novo PD patients using baseline WM structural connectivity from DTI data combined with clinical data.

2. Methods

2.1. Participants

All data in this study were obtained from the Parkinson's Progression Markers Initiative (PPMI) database (<https://www.ppmi-info.org/>). The PD patients chosen from the PPMI for the present study met the following inclusion criteria: (1) a diagnosis of PD for less than 2 years

and (2) untreated. The exclusion criteria were as follows: (1) lack of DTI or T1-weighted imaging (T1WI) data; (2) errors in image processing or poor image quality; (3) diagnosis of PD-MCI or PDD at baseline; (4) lack of follow-up neuropsychologic tests; and (5) development of PDD at follow-up (Fig. 1).

Ethical approval.

The PPMI trial (NCT01141023) was filed at [ClinicalTrials.gov](https://clinicaltrials.gov) and was granted ethical committee approval at all participating sites. Written informed consent was obtained from all participants before participation in the study.

2.2. Clinical assessment

The baseline clinical assessment included: (1) demographic variables (age, sex, education years, age of onset, duration of PD from diagnosis to enrollment, and family history of PD); (2) variables related to motor symptoms (Hoehn & Yahr stage, MDS-UPDRS Part II score, MDS-UPDRS Part III score, MDS-UPDRS total score, rigidity score, tremor score, tremor dominant/postural gait instability disorder classification, and Modified Schwab & England ADL score); (3) variables related to cognition (the Montreal Cognitive Assessment (MoCA) for global cognition; the Benton Judgment of Line Orientation (BJLO) for visuo-spatial function; the Hopkins Verbal Learning Test (HVLT discrimination recognition, HVLT immediate/total recall, HVLT retention, HVLT false alarms, HVLT delayed recall, HVLT delayed recognition for verbal memory); letter number sequencing (LNS) for working memory; symbol digit modalities test (SDMT) for attention-processing speed; and semantic fluency test (SFT) for verbal fluency); (4) variables related to other nonmotor symptoms (MDS-UPDRS Part I score, geriatric depression scale (GDS) score, STAI total score, SCOPA-AUT total score, Epworth sleepiness scale (ESS) score, REM sleep behavior disorder questionnaire score, and University of Pennsylvania Smell Identification Test (UPSIT) score). Patients were followed up for 5 years, and neuropsychologic tests were conducted at baseline and at each 1-year follow-up visit.

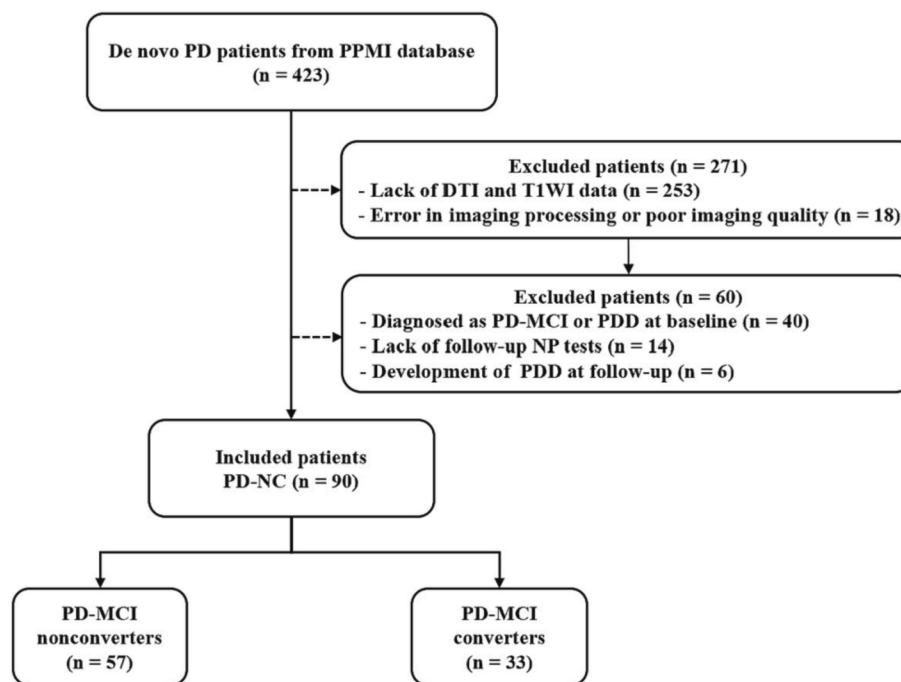


Fig. 1. Flowchart of patient inclusion. DTI, Diffusion tensor imaging; NP, neuropsychologic; PD-MCI, Parkinson's disease with mild cognitive impairment; PDD, Parkinson's disease dementia; PPMI, Parkinson's progression markers initiative; T1WI, T1-weighted imaging.

2.3. Diagnosis of PD-MCI

In this study, participants were classified as having PD-MCI according to the Movement Disorder Society (MDS) diagnostic criteria (Level I) (Litvan et al., 2012). Specifically, PD-MCI is defined as an MoCA score < 26 or 2 or more of the following cognitive tests with scores > 1.5 standard deviation (SD) below the standardized mean (HVLt total recall score ≤ 35 ; HVLt recognition discrimination score ≤ 35 ; Benton Judgment of Line Orientation score ≤ 6 ; letter number sequencing score ≤ 6 ; semantic fluency test score ≤ 35 ; or symbol digit modality test score ≤ 35).

Definition of PD-MCI converters: PD patients with normal cognition at baseline who subsequently developed PD-MCI within a 5-year follow-up.

Definition of PD-MCI nonconverters: PD with stable normal cognition at baseline and 5-year follow-up visits.

2.4. MRI acquisition and extraction of white matter features

All MRI examinations were performed using 3.0 T MRI scanners (Siemens Healthcare, USA) following a standard protocol. 3D T1-weighted images were obtained using a magnetization prepared rapid gradient echo (MPRAGE) sequence with the following parameters: repetition time (TR) = 2300 ms, echo time (TE) = 2.98 ms, voxel size = $1 \times 1 \times 1 \text{ mm}^3$, and flip angle = 9° . The diffusion-weighted images were obtained using an echo plane sequence with the following parameters: number of b0 images = 1, b-value = 1000 s/mm^2 , number of directions = 64, TR/TE = 900/80 ms, voxel size: $2 \times 2 \times 2 \text{ mm}^3$, and flip angle = 90° . More details are available at <https://www.ppmi-info.org/study-design/research-documents-and-sops/>.

We used a pipeline in the PANDA toolbox (Cui et al., 2013) (<https://www.nitrc.org/projects/panda>) based on the FMRIB Software Library (FSL), Octave and MATLAB's Pipeline System (PSOM), and Diffusion Toolkit and MRICron to analyze DTI data in MATLAB, using T1-weighted magnetic resonance imaging (MRI) data as anatomical references. First, we preprocessed the DTI data, including correction of head motion and eddy current distortions and removal of nonbrain tissues. To construct the brain network, we first used the fiber assignment by continuous tracking (FACT) algorithm to perform deterministic fiber tracking, setting the streamline to be terminated when it reached a voxel with an FA value < 0.2 or turned at an angle $< 45^\circ$. We defined the 210 cortical and 36 subcortical subregions segmented by the Brainnetome Atlas (Fan et al., 2016) as nodes and defined the average fiber length (FL), the fiber number (FN), and the average FA of fibers between two regions as edges. We finally obtained three 246×246 connectivity matrices, including the FL-weighted connectivity matrix, FN-weighted connectivity matrix and FA-weighted connectivity matrix. Considering that the values on both sides of the diagonal of the matrix are equal, we only took the values of the upper right corner of the matrix. In summary, we obtained $246 \times 246 / 2 \times 3 = 90774$ WM features based on the DTI data.

2.5. Feature selection

A total of 32 clinical variables and 90,774 structural connectivity metrics were obtained with the above steps. We divided these features into three categories: (1) clinical variables; (2) white matter variables (structural connectivity); and (3) clinical and white matter variables. For the structural connectivity metrics, we used a 50 % threshold to eliminate false-positive structural connectivity (i.e., a structural connectivity was considered a false-positive structural connectivity if 50 % of the individuals do not have that structural connectivity). We normalized each variable to zero mean and unit variance using the z score to reduce the effect of different units. And t tests and elastic net-based feature consensus ranking (ENFCR) were used to select features. First, in the training set, we used t tests to remove features without significant differences ($p > 0.01$) between groups. Then, we used ENFCR to reduce the

dimensionality of the features. The ENFCR algorithm includes multiple elastic nets, which can be used to identify features that contribute significantly to classification and rank the features according to the frequency with which they are selected (Yu et al., 2020b). Specifically, we randomly divided the PD patients into a training set (50 subjects, including 25 PD-MCI converters and 25 PD-MCI nonconverters) and a test set (40 subjects, including 32 PD-MCI converters and 8 PD-MCI nonconverters). To test the robustness, we also randomly divided the PD patients into a training set (46 subjects, including 23 PD-MCI converters and 23 PD-MCI nonconverters) and a test set (44 subjects, including 34 PD-MCI converters and 10 PD-MCI nonconverters). In the training test, we applied the ENFCR algorithm to select features in resampled 1000 training sets with the "bootstrap" algorithm. At last, all features were sorted from the most frequent to the least frequent selection in 1000 experiments. Features selected more than 500 times were considered as stable and important features for model construction (Shin et al., 2021). Overall, we believed that obtaining the frequency of each feature being selected in several repetitions of the experiment using the ENFCR algorithm to quantify the value of the feature can minimize data dependency and increase feature selection consistency.

2.6. Model construction and performance

To construct the model, we used four classifiers: linear discriminant analysis (LDA), support vector machine (SVM with linear kernel), K-nearest neighbor (KNN) and naïve Bayes (NB). We again used the above retained features in 1000 resampled training sets with the bootstrap algorithm for the four classifiers and evaluated model performance based on the test set. The model performance was evaluated using the area under the ROC curve (AUC), accuracy (ACC), sensitivity (SEN), and specificity (SPE). We also extracted the mean weight of selected features from SVM classifiers in 1000 resampled data sets.

2.7. Statistical analysis

SPSS software (version 26.0) was applied for statistical analyses of the clinical variables. The normality of the distributions was assessed using the Shapiro-Wilk (SW) test. Continuous variables with normal distributions are represented as the mean (standard deviation), and independent t tests were used to compare differences between groups. Continuous variables with abnormal distributions are represented as median (interquartile range), and Mann-Whitney U tests were used to compare differences between groups. Categorical variables are represented as percentages, and Chi-squared test were used to compare differences between groups. Significance was set at two tailed $p < 0.05$.

3. Results

3.1. Clinical characteristics

As shown in Fig. 1, in this study, 255 PD patients were excluded because of a lack of DTI and T1WI data, 18 PD patients were excluded because of image processing errors or poor image quality, 40 PD patients were excluded because of a diagnosis of PD-MCI or PDD, 14 PD patients were excluded because of a lack of follow-up neuropsychological (NP) tests, and 6 PD patients were excluded because of the development of PDD at follow-up, leaving 90 PD patients. 57 PD patients were identified as PD-MCI nonconverters, while 33 patients were identified as PD-MCI converters. The baseline clinical characteristics of the PD patients are listed in Table 1. The age, sex, MDS-UPDRS III score, HVLt discrimination recognition score, HVLt immediate/total recall score, HVLt retention score, HVLt false alarm score, HVLt delayed recall score, HVLt delayed recognition score, letter number sequencing score, semantic fluency total score, symbol digit modality score and MoCA score of the PD-MCI nonconverters and PD-MCI converters differed significantly. No significant differences were found in the years of education or

Table 1
Demographic and Clinical Characteristics.

Characteristic	PD-MCI	PD-MCI	P
	Nonconverters (n = 57)	Converters (n = 33)	
Age(years) ^a	55.9 (9.5)	64.7 (6.8)	< 0.001
Gender(male/female) ^b	33/24	20/13	0.508
Education(years) ^a	15.8 (2.6)	15.5 (3.2)	0.705
Benton Judgment of Line Orientation score ^c	14.0 (2.0)	13.0 (2.0)	0.290
MDS-UPDRS Part III score ^a	17.4 (7.0)	25.1 (10.7)	< 0.001
Geriatric Depression Scale score ^c	1.5 (2.3)	1.0 (3.0)	0.745
HVLT discrimination recognition ^c	11.0 (2.0)	10.0 (2.0)	0.001
HVLT immediate/total recall ^c	28.5 (4.1)	24.0 (5.0)	0.002
HVLT retention ^c	0.9 (0.2)	0.8 (0.2)	0.007
HVLT false alarms ^c	1.0 (1.3)	1.3 (2.0)	0.070
HVLT delayed recall ^c	10.0 (2.0)	9.0 (3.0)	0.002
HVLT delayed Recognition ^c	12.0 (1.0)	12.0 (1.0)	0.030
letter number sequencing score ^a	12.0 (2.7)	10.0 (2.3)	0.005
semantic fluency total score ^a	56.3 (9.7)	47.1 (8.9)	0.002
symbol digit modalities score ^a	45.7 (7.7)	41.7 (11.5)	0.025
MoCA score ^c	29.0 (2.0)	28.0 (2.0)	0.007

*P values were calculated with the Mann-whitney U test, independent t test or Chi-squared test appropriately.

^a Values are expressed as mean, with standard deviation in parentheses.

^b Values are expressed as proportion of male to female.

^c Values are expressed as median, with interquartile ranges in parentheses.

the Benton Judgment of Line Orientation score between the different groups.

3.2. Model performance

The model performance is summarized in Fig. 2. The models trained using clinical data showed moderate performance (AUC range: 0.62–0.68; ACC range: 0.63–0.77; SEN range: 0.45–0.66; SPE range: 0.64–0.84). Structural connectivity-trained models (AUC range, 0.81–0.84; ACC range, 0.75–0.86; SEN range, 0.77–0.91; SPE range, 0.71–0.88) performed like models that were trained with clinical data as well as structural connectivity (AUC range, 0.81–0.85; ACC range, 0.74–0.85; SEN range, 0.79–0.91; SPE range, 0.70–0.89). Additionally, the model performance of the division of training set and test set of 7:3 of PD-MCI converters was only slightly reduced (Supplementary Table S1).

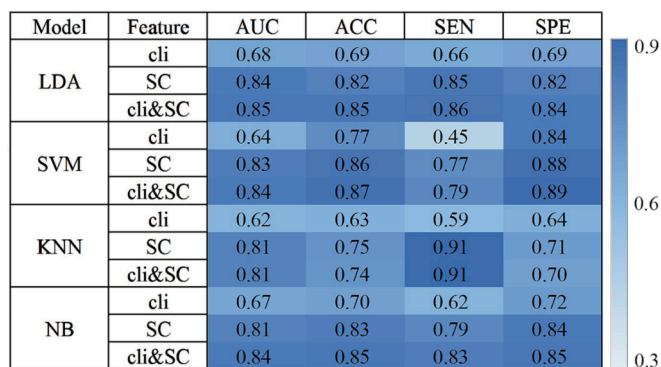


Fig. 2. Heat maps of areas under the receiver operating characteristic curve, accuracy, sensitivity and specificity from four machine learning models to predict Parkinson’s disease with mild cognitive impairment conversion. ACC, accuracy; AUC, areas under the receiver operating characteristic curve; cli, clinical data; KNN, k-nearest neighbor; LDA, linear discriminant analysis; NB, naive bayes; SC, structural connectivity; SEN, sensitivity; SPE, specificity; SVM, support vector machine.

3.3. Feature selection

The features selected in the models are shown in Fig. 3 and Fig. 4. Whether clinical data alone or clinical data combined with structural connectivity data were used to construct PD-MCI prediction models, the MDS-UPDRS III score was selected among the clinical variables. Age was selected in the model trained with only clinical data. Nine structural connectivity features were selected in the models trained with structural connectivity data and the models trained with both clinical and structural connectivity data, including the mean fiber length (FL) between caudal area 45 in the left inferior frontal gyrus (IFG.L.A45c) and opercular area 44 in the left inferior frontal gyrus (IFG.L.A44op), the mean FL between opercular area 44 in the right inferior frontal gyrus (IFG.R.A44op) and right dorsal agranular insula (INS.R.dIa), the mean FL between area 1/2/3 (tongue and larynx region) in the right postcentral gyrus (PoG.R.A1/2/3tonIa) and right dorsal agranular insula (INS.R.dIa), the mean fractional anisotropy (FA) between postcentral area 7 in the left superior parietal lobule (SPL.L.A7pc) and medial area 5 (PEm) in the left precuneus (Pcun.L.A5m), the mean fiber number (FN) between medial area 11 in the right orbital gyrus (OrG.R.A11m) and the ventral caudate in the right basal ganglia (BG.R.vCa), the mean FN between the left caudal hippocampus (Hipp.L.cHipp) and left caudal temporal thalamus (Tha.L.cTha), the mean FL between rostradorsal area 40 (PFt) in the right inferior parietal lobule (IPL.R.A40rd) and area 2 in the right postcentral gyrus (PoG.R.A2), the FL between the caudal cuneus gyrus in the left medioventral occipital cortex (MVOcC.L.cCunG) and medial superior occipital gyrus in the left lateral occipital cortex (LOcC.L.msOccG), and the FL between dorsal area 9/46 in the left middle frontal gyrus (MFG.L.A9/46d) and ventral area 9/46 in the left middle frontal gyrus (MFG.L.A9/46v). The mean FL between the occipital polar cortex in the right lateral occipital cortex (LOcC.R.OPC) and inferior occipital gyrus in the right lateral occipital cortex (LOcC.R.iOccG), the mean FL between the dorsal caudate in the left basal ganglia (BG.L.dCa) and left posterior parietal thalamus (Tha.L.Pptha) and the mean FA between rostral area 21 in the left middle temporal gyrus (MTG.L.A21r) and intermediate lateral area 20 in the left inferior temporal gyrus (ITG.L.A20il) were selected only for the model trained with structural connectivity features. Feature weight in the SVM classifier are summarized in Supplementary Table S2. The MDS-UPDRS III score, age, the mean FL between the LOcC.R.OPC and LOcC.R.iOccG, the mean FL between the BG.L.dCa and Tha.L.Pptha showed positive weights, indicating that patients with higher values had higher possibilities of PD-MCI conversion. In contrast, other structural connectivity features showed negative weights, indicating that patients with lower values had higher possibilities of PD-MCI conversion.

4. Discussion

In summary, our research showed that by utilizing machine learning, baseline WM structural connectivity features could be used to predict future conversion to PD-MCI in de novo PD-NC patients at an individual level. The models trained using clinical data showed moderate performance (AUC range: 0.62–0.68; ACC range: 0.63–0.77; SEN range: 0.45–0.66; SPE range: 0.64–0.84). Models trained based on structural connectivity features (AUC range, 0.81–0.84; ACC range, 0.75–0.86; SEN range, 0.77–0.91; SPE range, 0.71–0.88) performed similarly to models that were trained with clinical data and structural connectivity features (AUC range, 0.81–0.85; ACC range, 0.74–0.85; SEN range, 0.79–0.91; SPE range, 0.70–0.89). Furthermore, our findings may reveal the pathophysiology of PD-MCI conversion by confirming the structural connectivity among various brain regions in the frontal lobe, parietal lobe, occipital lobe, temporal lobe, insula, and subcortical nuclei as important features.

In line with previous studies (Schrug et al., 2017; Siciliano et al., 2017), our study showed that the baseline MDS-UPDRS III score and age are important predictors of cognitive impairment in patients with PD.

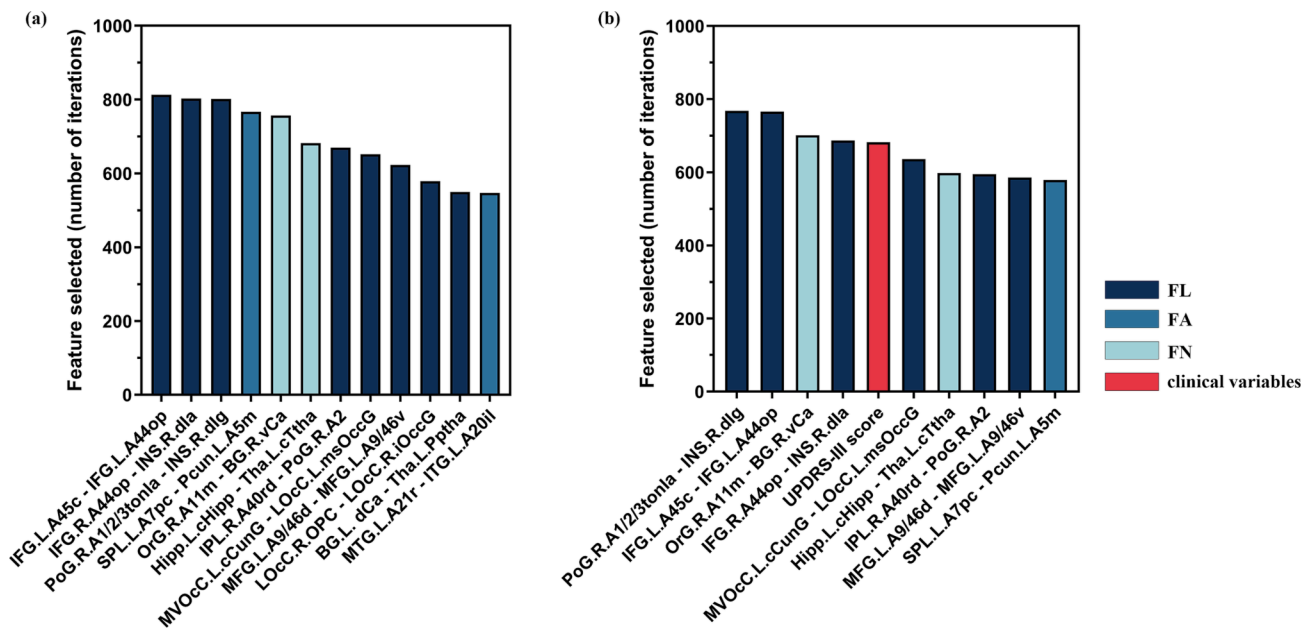


Fig. 3. Bar charts show the frequency of features selected for classification of Parkinson's disease with mild cognitive impairment converters and nonconverters. (a) Features of structural connectivity only. (b) Features of both clinical data and structural connectivity. L, left; R, right; IFG, inferior frontal gyrus; A45c, caudal area 45; A44op, opercular area 44; INS, insular gyrus; dia, dorsal agranular insula; PoG, postcentral gyrus; A1/2/3tonla, area 1/2/3(tongue and larynx region); dig, dorsal granular insula; SPL, superior parietal lobule; A7pc, postcentral area 7; PCun, precuneus; A5m, medial area 5; OrG, orbital gyrus; A11m, medial area 11; BG, basal ganglia; vCa, ventral caudate; cHipp, caudal hippocampus; cTtha, caudal temporal thalamus; IPL, inferior parietal lobule; A40rd, rostrorodorsal area 40; A2, area 2; MVOCc, medioventral occipital cortex; cCunG, caudal cuneus gyrus; LOcC, lateral occipital cortex; msOccG, medial superior occipital gyrus; MFG, middle temporal gyrus; A9/46d, dorsal area 9/46; A9/46v, ventral area 9/46; OPC, occipital polar cortex; iOccG, inferior occipital gyrus; dCa, dorsal caudate; Pptha, posterior parietal thalamus; MTG, middle temporal gyrus; A21r, rostral area 21; ITG, inferior temporal gyrus; A20il, intermediate lateral area 20.

Harvey et al. indicated that baseline cognitive-related scores are helpful for predicting cognitive state changes in patients with PD using PPMI data (Harvey et al., 2022). However, although some baseline cognitive variables ranked high according to the feature ordering in our study, these features were selected less than 500 times in 1000 experiments. We surmised that this is because Harvey's study included both PD-MCI and PDD converters, whereas our analysis included only PD-MCI converters. Phongpreecha et al. also discovered that while cognitive testing was the most important predictor of future PDD conversion, it could not reliably predict PD-MCI conversion (Phongpreecha et al., 2020). Moreover, larger sample sizes should be considered in the future to verify our findings.

In our study, features were selected in the inferior frontal gyrus, middle frontal gyrus, orbital frontal gyrus, caudate nucleus, and thalamus. The frontal lobe, caudate nucleus and thalamus are thought to be involved in a variety of important cognitive functions (Li et al., 2022; Manza et al., 2016; Suo et al., 2019). Moreover, previous studies have indicated that the cortico-striatal-thalamo-cortical loop plays an important role in executive functions (Shang et al., 2020). Furthermore, ^{18}F -fluorodeoxyglucose (^{18}F -FDG) uptake in the inferior frontal gyrus is positively correlated with executive function (Han et al., 2021). The results of a longitudinal study showed that the cerebral blood flow (CBF) in the left lateral orbitofrontal cortex was significantly reduced in patients that converted to PD-MCI compared to that in nonconverters, suggesting that reduced longitudinal CBF in the orbitofrontal lobe may affect cognitive function in patients with PD (Wang et al., 2022).

The insula is highly connected to and interacts with several brain regions (e.g., the basal ganglia and frontal, parietal, and temporal cortices) and thus plays a central role in various cognitive processes (Li et al., 2022). The results of a longitudinal study showed that a significant reduction in gray matter density in the left insula at baseline could potentially be a predictor of eventual dementia in PD-MCI patients (Lee et al., 2014). Furthermore, ^{18}F -FDG uptake and executive function in the insula were found to be significantly associated in PD patients (Han

et al., 2021). The extent of Lewy body accumulation in the hippocampus is linked to the severity of cognitive impairment in patients with PD (Hall et al., 2014). The atrophy of hippocampal subregions may be an important biomarker for predicting PD-NC to PD-MCI conversion (Xu et al., 2023). Moreover, the MD value of the hippocampus, an important feature in identifying PD-NC and PD-MCI patients, is significantly negatively correlated with the MoCA score (Chen et al., 2023).

The precuneus and inferior parietal lobule are critical nodes in the default mode network (DMN) that play essential roles in cognitive processing (Ruppert et al., 2021). Increased hypometabolism in the precuneus is associated with increased cognitive decline in patients with PD, and baseline precuneus gyrus cerebral fluorodeoxyglucose-PET (FDG-PET) data could be used to differentiate between PDD converters and stable PD-MCI patients (Booth et al., 2022). The IPL is engaged in a wide range of cognitive tasks, including spatial attention, language processing, and recall of situational memory (Xing et al., 2021). Reduced functional connectivity in the bilateral inferior parietal lobule in PD patients is significantly correlated with various cognitive parameters (Tessitore et al., 2012).

In addition, in our study, features were selected in the occipital and temporal areas, including the cuneus, superior occipital gyrus, inferior occipital gyrus, middle temporal gyrus and inferior temporal gyrus. The occipital lobe is critical for memory-related visuospatial information processing, and the MOG is an integral part of the visual cortex (Xing et al., 2021). Occipital cortical atrophy has been linked to hallucinations in patients with PD, and aberrant hallucinations may enhance susceptibility to cognitive impairment (Xia et al., 2013). The inferior temporal gyrus is the final part of the ventral visual pathway, and temporal lobe atrophy is associated with impaired visuospatial abilities in patients with PDD (Rektorova et al., 2014).

Our study had some limitations. Firstly, the sample size of this study was limited due to the specificity of the subjects (new diagnosis, 5 years of follow-up), although we used 1000 times bootstrap and different classifiers to evaluate our findings. In future work, larger sample sizes

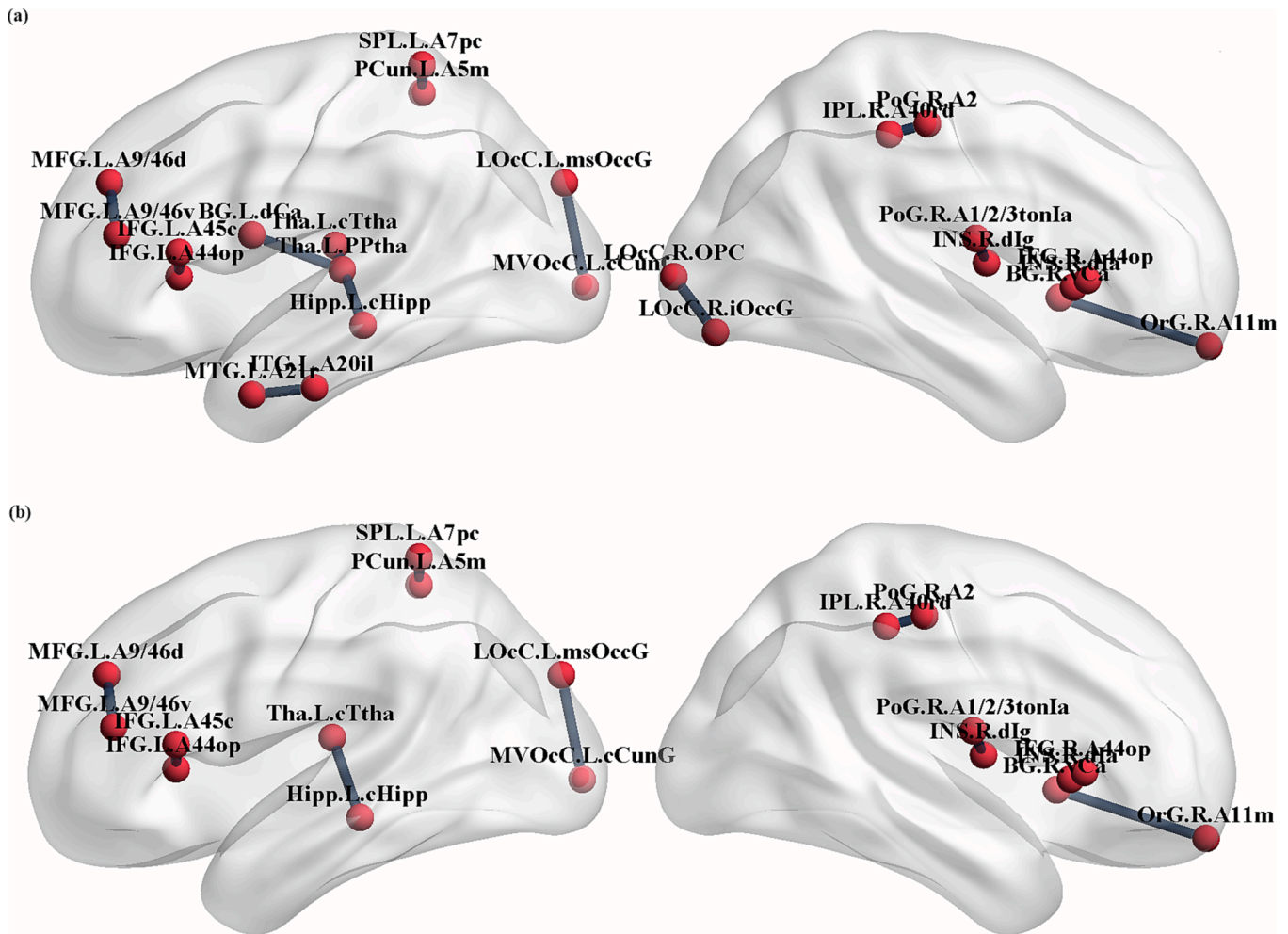


Fig. 4. The distribution of structural connectivity features according to different combinations. (a) Features of structural connectivity only. (b) Features of both clinical data and structural connectivity. L, left; R, right; IFG, inferior frontal gyrus; A45c, caudal area 45; A44op, opercular area 44; INS, insular gyrus; dia, dorsal agranular insula; PoG, postcentral gyrus; A1/2/3tonla, area 1/2/3(tongue and larynx region); dlG, dorsal granular insula; SPL, superior parietal lobule; A7pc, postcentral area 7; Pcu, precuneus; A5m, medial area 5; OrG, orbital gyrus; A11m, medial area 11; BG, basal ganglia; vCa, ventral caudate; cHipp, caudal hippocampus; cTha, caudal temporal thalamus; IPL, inferior parietal lobule; A40rd, rostradorsal area 40; A2, area 2; MVOcC, medioventral occipital cortex; cCunG, caudal cuneus gyrus; LOcC, lateral occipital cortex; msOccG, medial superior occipital gyrus; MFG, middle temporal gyrus; A9/46d, dorsal area 9/46; A9/46v, ventral area 9/46; OPC, occipital polar cortex; iOccG, inferior occipital gyrus; dCa, dorsal caudate; Pptha, posterior parietal thalamus; MTG, middle temporal gyrus; A21r, rostral area 21; ITG, inferior temporal gyrus; A20il, intermediate lateral area 20.

should be used to validate these findings. Second, because the PPMI is a cohort of PD patients with de novo disease and that its cognitive scale differs from that used in other studies, there is no feasible external cohort similar to the PPMI to validate our findings. Third, the use of MDS level I scores instead of level II diagnosis criteria in the PPMI cohort to diagnose PD-MCI may result in incorrect diagnoses. Finally, patients received treatment during the follow-up period, which may interfere with the cognition diagnosis.

CRediT authorship contribution statement

Xiaofei Huang: Conceptualization, Investigation, Writing – original draft, Writing – review & editing. **Qing He:** Methodology, Writing – original draft. **Xiuhang Ruan:** Data curation, Methodology, Validation. **Yuting Li:** Formal analysis, Methodology, Visualization. **Zhanyu Kuang:** Data curation, Formal analysis. **Mengfan Wang:** Data curation, Formal analysis. **Riyu Guo:** Data curation, Formal analysis. **Shuwen Bu:** Data curation, Formal analysis. **Zhaoxiu Wang:** Data curation, Formal analysis. **Shaode Yu:** Methodology, Validation. **Amei Chen:** Conceptualization, Funding acquisition, Supervision, Writing – review & editing. **Xinhua Wei:** .

Declaration of competing interest

The authors declare that they have no known competing financial interests or personal relationships that could have appeared to influence the work reported in this paper.

Data availability

The authors do not have permission to share data.

Acknowledgements

This work was supported by the Natural Science Foundation of Guangdong Province (No. 2021A1515011288, No.2023A1515010606), Guangdong Medical Research Foundation (A2022263).

Appendix A. Supplementary data

Supplementary data to this article can be found online at <https://doi.org/10.1016/j.nicl.2023.103548>.

References

- Aarsland, D., Creese, B., Politis, M., Chaudhuri, K.R., Ffytche, D.H., Weintraub, D., Ballard, C., 2017. Cognitive decline in Parkinson disease. *Nature Reviews. Neurology* 13, 217–231.
- Booth, S., Park, K.W., Lee, C.S., Ko, J.H., 2022. Predicting cognitive decline in Parkinson's disease using FDG-PET-based supervised learning. *J Clin Invest* 132.
- Burke, R.E., O'Malley, K., 2013. Axon degeneration in Parkinson's disease. *Exp Neurol* 246, 72–83.
- Caspell-Garcia, C., Simuni, T., Tosun-Turgut, D., Wu, I.W., Zhang, Y., Nalls, M., Singleton, A., Shaw, L.A., Kang, J.H., Trojanowski, J.Q., Siderowf, A., Coffey, C., Lasch, S., Aarsland, D., Burn, D., Chahine, L.M., Espay, A.J., Foster, E.D., Hawkins, K.A., Litvan, I., Richard, I., Weintraub, D., 2017. Multiple modality biomarker prediction of cognitive impairment in prospectively followed de novo Parkinson disease. *PLoS One* 12, e0175674.
- Caviness, J.N., Driver-Dunckley, E., Connor, D.J., Sabbagh, M.N., Hentz, J.G., Noble, B., Evidente, V.G., Shill, H.A., Adler, C.H., 2007. Defining mild cognitive impairment in Parkinson's disease. *Movement Disorders : Official Journal of the Movement Disorder Society* 22, 1272–1277.
- Chen, B., Xu, M., Yu, H., He, J., Li, Y., Song, D., Fan, G.G., 2023. Detection of mild cognitive impairment in Parkinson's disease using gradient boosting decision tree models based on multilevel DTI indices. *J Transl Med* 21, 310.
- Cui, Z., Zhong, S., Xu, P., He, Y., Gong, G., 2013. PANDA: a pipeline toolbox for analyzing brain diffusion images. *Frontiers in Human Neuroscience* 7, 42.
- Delgado-Alvarado, M., Gago, B., Navalpotro-Gomez, I., Jiménez-Urbiet, H., Rodriguez-Oroz, M.C., 2016. Biomarkers for dementia and mild cognitive impairment in Parkinson's disease. *Movement Disorders : Official Journal of the Movement Disorder Society* 31, 861–881.
- Fan, L., Li, H., Zhuo, J., Zhang, Y., Wang, J., Chen, L., Yang, Z., Chu, C., Xie, S., Laird, A.R., Fox, P.T., Eickhoff, S.B., Yu, C., Jiang, T., 2016. The Human Brainnetome Atlas: A New Brain Atlas Based on Connectonal Architecture. *Cerebral cortex (New York, N. Y. : 1991)* 26, 3508–3526.
- Filippi, M., Canu, E., Donzuso, G., Stojkovic, T., Basaia, S., Stankovic, I., Tomić, A., Marković, V., Petrović, I., Stefanova, E., Kostić, V.S., Agosta, F., 2020. Tracking Cortical Changes Throughout Cognitive Decline in Parkinson's Disease. *Movement Disorders : Official Journal of the Movement Disorder Society* 35, 1987–1998.
- Foo, H., Mak, E., Chander, R.J., Ng, A., Au, W.L., Sitoh, Y.Y., Tan, L.C., Kandiah, N., 2017. Associations of hippocampal subfields in the progression of cognitive decline related to Parkinson's disease. *NeuroImage. Clinical* 14, 37–42.
- Hall, H., Reyes, S., Landeck, N., Bye, C., Leanza, G., Double, K., Thompson, L., Halliday, G., Kirik, D., 2014. Hippocampal Lewy pathology and cholinergic dysfunction are associated with dementia in Parkinson's disease. *Brain : a Journal of Neurology* 137, 2493–2508.
- Han, L., Lu, J., Tang, Y., Fan, Y., Chen, Q., Li, L., Liu, F., Wang, J., Zuo, C., Zhao, J., 2021. Dopaminergic and Metabolic Correlations With Cognitive Domains in Non-demented Parkinson's Disease. *Frontiers in Aging Neuroscience* 13, 627356.
- Harvey, J., Reijnders, R.A., Cavill, R., Duits, A., Köhler, S., Eijssen, L., Rutten, B.P.F., Shireby, G., Torkamani, A., Creese, B., Leentjens, A.F.G., Lunnon, K., Pishva, E., 2022. Machine learning-based prediction of cognitive outcomes in de novo Parkinson's disease. *NPJ Parkinsons Dis* 8, 150.
- Hely, M.A., Reid, W.G., Adena, M.A., Halliday, G.M., Morris, J.G., 2008. The Sydney multicenter study of Parkinson's disease: the inevitability of dementia at 20 years. *Movement Disorders : Official Journal of the Movement Disorder Society* 23, 837–844.
- Huang, W., Li, X., Li, X., Kang, G., Han, Y., Shu, N., 2021. Combined Support Vector Machine Classifier and Brain Structural Network Features for the Individual Classification of Amnesic Mild Cognitive Impairment and Subjective Cognitive Decline Patients. *Frontiers in Aging Neuroscience* 13, 687927.
- Kurowska, Z., Kordower, J.H., Stoessl, A.J., Burke, R.E., Brundin, P., Yue, Z., Brady, S.T., Milbrandt, J., Trapp, B.D., Sherer, T.B., Medicetty, S., 2016. Is Axonal Degeneration a Key Early Event in Parkinson's Disease? *J Parkinsons Dis* 6, 703–707.
- Lee, J.E., Cho, K.H., Song, S.K., Kim, H.J., Lee, H.S., Sohn, Y.H., Lee, P.H., 2014. Exploratory analysis of neuropsychological and neuroanatomical correlates of progressive mild cognitive impairment in Parkinson's disease. *J Neurol Neurosurg Psychiatry* 85, 7–16.
- Li, L., Ji, B., Zhao, T., Cui, X., Chen, J., Wang, Z., 2022. The structural changes of gray matter in Parkinson disease patients with mild cognitive impairments. *PLoS One* 17, e0269787.
- Lin, H., Liu, Z., Yan, W., Zhang, D., Liu, J., Xu, B., Li, W., Zhang, Q., Cai, X., 2021. Brain connectivity markers in advanced Parkinson's disease for predicting mild cognitive impairment. *Eur Radiol* 31, 9324–9334.
- Litvan, I., Goldman, J.G., Tröster, A.L., Schmand, B.A., Weintraub, D., Petersen, R.C., Mollenhauer, B., Adler, C.H., Marder, K., Williams-Gray, C.H., Aarsland, D., Kulisevsky, J., Rodriguez-Oroz, M.C., Burn, D.J., Barker, R.A., Emre, M., 2012. Diagnostic criteria for mild cognitive impairment in Parkinson's disease: Movement Disorder Society Task Force guidelines. *Movement Disorders : Official Journal of the Movement Disorder Society* 27, 349–356.
- Manza, P., Zhang, S., Li, C.S., Leung, H.C., 2016. Resting-state functional connectivity of the striatum in early-stage Parkinson's disease: Cognitive decline and motor symptomatology. *Hum Brain Mapp* 37, 648–662.
- Mei, J., Desrosiers, C., Frasnelli, J., 2021. Machine Learning for the Diagnosis of Parkinson's Disease: A Review of Literature. *Frontiers in Aging Neuroscience* 13, 633752.
- Park, C.H., Shin, N.Y., Yoo, S.W., Seo, H., Yoon, U., Yoo, J.Y., Ahn, K., Kim, J.S., 2022. Simulating the progression of brain structural alterations in Parkinson's disease. *NPJ Parkinsons Dis* 8, 86.
- Phongpreecha, T., Cholerton, B., Mata, I.F., Zabetian, C.P., Poston, K.L., Aghaepour, N., Tian, L., Quinn, J.F., Chung, K.A., Hiller, A.L., Hu, S.-C., Edwards, K.L., Montine, T. J., 2020. Multivariate prediction of dementia in Parkinson's disease. *NPJ Parkinsons Dis* 6, 20.
- Pigott, K., Rick, J., Xie, S.X., Hurtig, H., Chen-Plotkin, A., Duda, J.E., Morley, J.F., Chahine, L.M., Dahodwala, N., Akhtar, R.S., Siderowf, A., Trojanowski, J.Q., Weintraub, D., 2015. Longitudinal study of normal cognition in Parkinson disease. *Neurology* 85, 1276–1282.
- Rektor, I., Svátková, A., Vojtšek, L., Zikmundová, I., Vaníček, J., Király, A., Szabó, N., 2018. White matter alterations in Parkinson's disease with normal cognition precede grey matter atrophy. *PLoS One* 13, e0187939.
- Rektorova, I., Biundo, R., Marecek, R., Weis, L., Aarsland, D., Antonini, A., 2014. Grey matter changes in cognitively impaired Parkinson's disease patients. *PLoS One* 9, e85595.
- Ruppert, M.C., Greuel, A., Freigang, J., Tahmasian, M., Maier, F., Hammes, J., van Eimeren, T., Timmermann, L., Tittgemeyer, M., Drzezga, A., Eggers, C., 2021. The default mode network and cognition in Parkinson's disease: A multimodal resting-state network approach. *Hum Brain Mapp* 42, 2623–2641.
- Schrag, A., Siddiqui, U.F., Anastasiou, Z., Weintraub, D., Schott, J.M., 2017. Clinical variables and biomarkers in prediction of cognitive impairment in patients with newly diagnosed Parkinson's disease: a cohort study. *The Lancet. Neurology* 16, 66–75.
- Shang, S., Chen, Y.C., Zhang, H., Dou, W., Qian, L., Yin, X., Wu, J., 2020. Mapping the Interactive Effects of ApoE Gene Polymorphism on Caudate Functional Connectivity in Mild Cognitive Impairment Associated With Parkinson's Disease. *Frontiers in Neuroscience* 14, 857.
- Shin, N.-Y., Bang, M., Yoo, S.-W., Kim, J.-S., Yun, E., Yoon, U., Han, K., Ahn, K.J., Lee, S.-K., 2021. Cortical Thickness from MRI to Predict Conversion from Mild Cognitive Impairment to Dementia in Parkinson Disease: A Machine Learning-based Model. *Radiology* 300, 390–399.
- Siciliano, M., De Micco, R., Trojano, L., De Stefano, M., Baiano, C., Passaniti, C., De Mase, A., Russo, A., Tedeschi, G., Tessitore, A., 2017. Cognitive impairment is associated with Hoehn and Yahr stages in early, de novo Parkinson disease patients. *Parkinsonism & Related Disorders* 41, 86–91.
- Suo, X., Lei, D., Cheng, L., Li, N., Zuo, P., Wang, D.J.J., Huang, X., Lui, S., Kemp, G.J., Peng, R., Gong, Q., 2019. Multidelay multiparametric arterial spin labeling perfusion MRI and mild cognitive impairment in early stage Parkinson's disease. *Hum Brain Mapp* 40, 1317–1327.
- Tessitore, A., Esposito, F., Vitale, C., Santangelo, G., Amboni, M., Russo, A., Corbo, D., Cirillo, G., Barone, P., Tedeschi, G., 2012. Default-mode network connectivity in cognitively unimpaired patients with Parkinson disease. *Neurology* 79, 2226–2232.
- Thiebaut de Schotten, M., Forkel, S.J., 2022. The Emergent Properties of the Connected Brain 378, 505–510.
- Wang, J., Zhang, W., Zhou, Y., Jia, J., Li, Y., Liu, K., Ye, Z., Jin, L., 2022. Altered Prefrontal Blood Flow Related With Mild Cognitive Impairment in Parkinson's Disease: A Longitudinal Study. *Frontiers in Aging Neuroscience* 14, 896191.
- Weintraub, D., Burn, D.J., 2011. Parkinson's disease: the quintessential neuropsychiatric disorder. *Movement Disorders : Official Journal of the Movement Disorder Society* 26, 1022–1031.
- Xia, J., Miu, J., Ding, H., Wang, X., Chen, H., Wang, J., Wu, J., Zhao, J., Huang, H., Tian, W., 2013. Changes of brain gray matter structure in Parkinson's disease patients with dementia. *Neural Regen Res* 8, 1276–1285.
- Xing, Y., Fu, S., Li, M., Ma, X., Liu, M., Liu, X., Huang, Y., Xu, G., Jiao, Y., Wu, H., Jiang, G., Tian, J., 2021. Regional Neural Activity Changes in Parkinson's Disease-Associated Mild Cognitive Impairment and Cognitively Normal Patients. *Neuropsychiatr Dis Treat* 17, 2697–2706.
- Xu, H., Liu, Y., Wang, L., Zeng, X., Xu, Y., Wang, Z., 2023. Role of hippocampal subfields in neurodegenerative disease progression analyzed with a multi-scale attention-based network. *NeuroImage. Clinical* 38, 103370.
- Yau, Y., Zeighami, Y., Baker, T.E., Larcher, K., Vainik, U., Dadar, M., Fonov, V.S., Hagmann, P., Griffa, A., Misić, B., Collins, D.L., Dagher, A., 2018. Network connectivity determines cortical thinning in early Parkinson's disease progression. *Nat Commun* 9, 12.
- Yu, J., Rawtaer, I., Fam, J., Feng, L., Kua, E.H., Mahendran, R., 2020a. The individualized prediction of cognitive test scores in mild cognitive impairment using structural and functional connectivity features. *NeuroImage* 223, 117310.
- Yu, S., Chen, H., Yu, H., Zhang, Z., Liang, X., Qin, W., Xie, Y., Shi, P., 2020b. Elastic Net based Feature Ranking and Selection. *arXiv preprint arXiv:2012.14982*.
- Zhou, C., Guan, X.J., Guo, T., Zeng, Q.L., Gao, T., Huang, P.Y., Xuan, M., Gu, Q.Q., Xu, X. J., Zhang, M.M., 2020. Progressive brain atrophy in Parkinson's disease patients who convert to mild cognitive impairment. *CNS Neurosci Ther* 26, 117–125.